Performance of the Gemini near-infrared spectrograph

Jonathan H. Elias[a], Bernadette Rodgers[b], Richard R. Joyce[a], Manuel Lazo[b], Gregory Doppmann[b], Claudia Winge[b], and Alberto Rodríguez-Ardila[c]
[a]National Optical Astronomy Observatory, 950 N. Cherry Ave., Tucson, AZ 85719
[b]Gemini Observatory, Casilla 603, La Serena, Chile
[c]Laboratório Nacional de Astrofísica, R. Estados Unidos 154, Itajubá-MG, Brazil, 37504-364

ABSTRACT

The Gemini Near-Infrared Spectrograph (GNIRS) has been in successful use on the Gemini South 8-m telescope for over two years. We describe the performance of the instrument and discuss how it matches the expectations from the design. We also examine the lessons to be learned regarding the design and operation of similar large cryogenic facility instruments.

Keywords: infrared spectrograph, Gemini telescope

1. INTRODUCTION

The Gemini Near-Infrared Spectrograph (GNIRS) was intended to be one of the "workhorse" instruments for the Gemini 8-m telescopes[1]. It was completed in late 2003 and commissioned during the period October 2003 to April 2004, and began routine science use at the Gemini South telescope in semester 2004B.

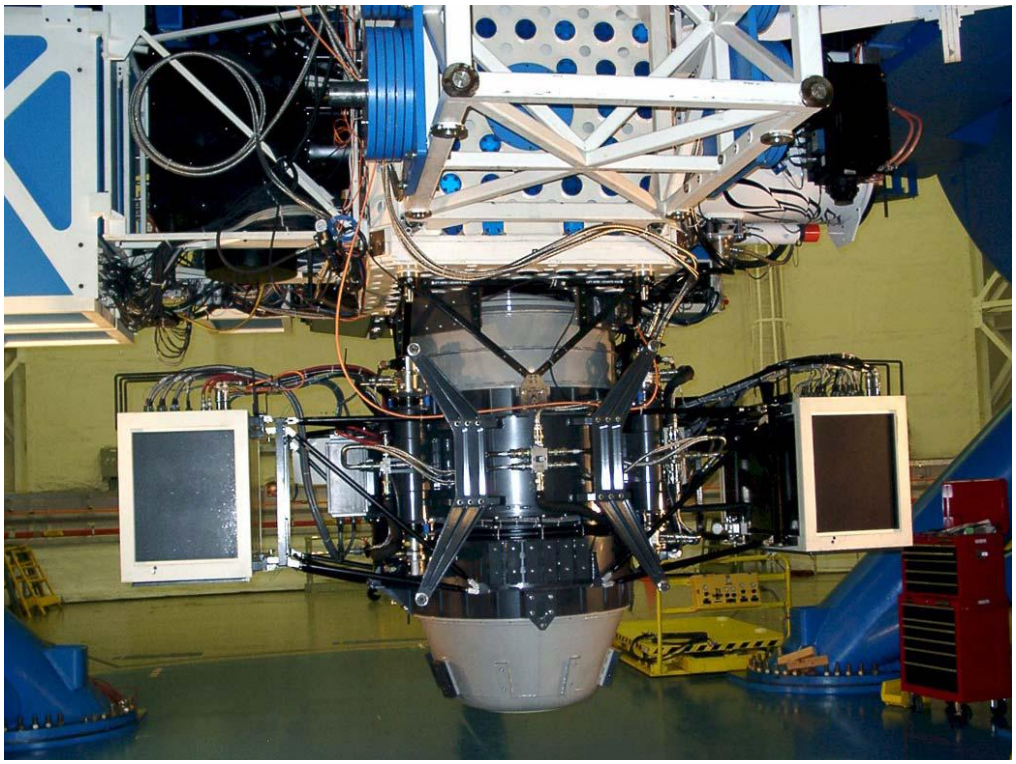

Figure 1. GNIRS installed on the up-looking port on the Gemini South telescope in December 2003. The instrument is normally installed on one of the side ports, for example at the location of the dummy instrument (white framework) at the top of the picture.

Ground-based and Airborne Instrumentation for Astronomy, edited by Ian S. McLean, Masanori Iye,
Proc. of SPIE Vol. 6269, 626914, (2006) · 0277-786X/06/$15 · doi: 10.1117/12.671765

In this paper, we describe the performance of GNIRS and discuss what can be learned from two years of extensive operation. The design of GNIRS is described elsewhere ([2], see also [3-9]), but specifications are summarized below:

- Wavelength coverage from 1-5.5 μm.
- Two pixel scales, of approximately 0.05 and 0.15 arcsec/pixel. The smaller pixel scale was intended both for use in exceptional seeing conditions, and with an adaptive optics (AO) system.
- Two spectral resolutions. The lowest spectral resolution was intended to cover a single atmospheric "window" on the detector, which was specified as an ALADDIN III 1k x 1k InSb array[3,5]. This implied a resolving power ($\lambda/\Delta\lambda$) of ~1700. The second spectral resolution was intended to permit useful work in between atmospheric airglow lines. A resolving power of ~6000 was adopted, although higher values were considered. These resolving powers were intended to be available for both pixel scales; the design adopted also provides a still higher resolving power (~18,000) with the 0.05 arcsec pixel scale.
- A long slit mode of 50 arcsec or greater.
- A polarization analysis mode.
- An integral field unit (IFU), which maps a rectangular field onto a long slit or equivalent; this is described in detail in [6,7].
- A cross-dispersed mode, which provides coverage of multiple windows in the R~1700 mode, thus providing complete coverage of 0.8-2.5 μm, though with a short slit. This mode also provides partial coverage of each order over the same wavelength region, using the higher-resolution grating.
- A near-infrared on-instrument wavefront sensor (OIWFS)[3,4], capable of providing guiding and focus referenced to a location close to the instrument input. This was intended as a substitute for the telescope's peripheral wavefront sensors (PWFS). The OIWFS would, in theory, provide better flexure correction and would also provide the ability to work in obscured regions devoid of visible stars suitable for the PWFS.

GNIRS was originally intended to be deployed to the Gemini North telescope, but during the late stages of construction it was decided to send it to Gemini South instead. As a result, it is not currently used with an adaptive optics system; it may be AO-fed at some point in the future, either at Gemini North or Gemini South. A fairly detailed description of GNIRS and its operation can be found at [10].

2. PERFORMANCE

We discuss first the operation of the spectrograph, and then provide some qualitative information on performance.

2.1 Operation

The Gemini telescopes are operated in both queue and classical modes, but from the perspective of the observer at the telescope actually operating the instrument, there is little difference between the two modes. That is, although the processes leading to selection of the specific science target are quite different, the procedures once the target is selected are essentially the same.

One real difference is that a classical night is more likely to make use of a small number of configurations - potentially no more than one - whereas it is common for queue observations to use a different configuration for each science target. This leads to slightly greater overhead in night-time calibrations, since it is less likely that two queue targets will be able to use the same calibration observations.

The basic observing sequence comprises three parts: acquisition, science data acquisition, and calibration. A detailed discussion of observing procedures and observation preparation can be found at the Gemini website[10].

2.1.1 Acquisition

The spectrograph contains a mirror that can be inserted in the collimated beam to bypass the dispersers and send light directly to the camera (see [2]). This produces an image of the sky viewed through the filters and slit or IFU (see Figure 2 for an example). Using an image taken with the desired slit for reference and an image taken through an “open”

position, it is possible to identify and center the object on the slit. The GNIRS design has the advantage that the dispersing elements (grating and prism) do not have to be moved to do acquisition, allowing them to remain fixed between the science target and the calibration star, or between multiple science observations.

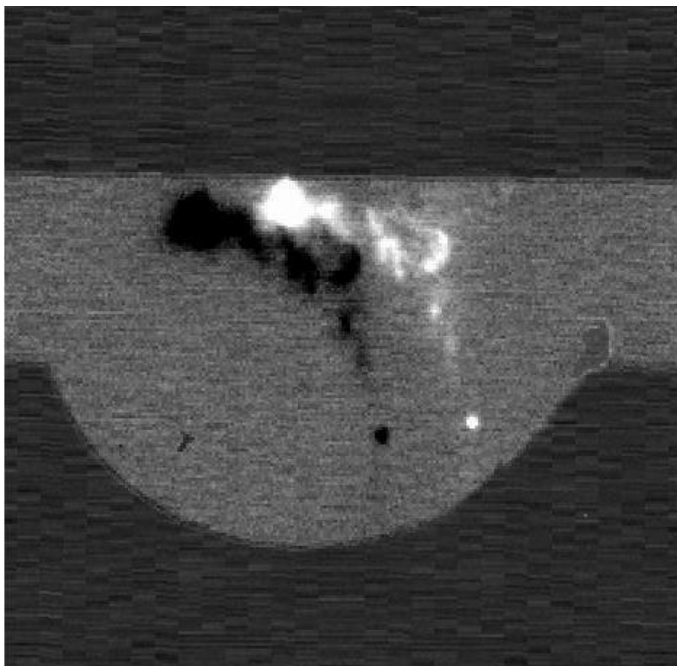

Figure 2. Acquisition image. The figure shows a sky-subtracted image of the Herbig-Haro object HH48, produced by differencing two images taken with the telescope moved a few arcseconds on the sky. The full acquisition field extends 100 arcseconds along the slit (beyond the limits of this figure); the width is 10 arcseconds plus an additional semi-circle of 15 arcseconds radius.

Acquisition is normally carried out using the filter for 4th order, which approximates the standard H filter, but any filter can be used. It is sometimes necessary to acquire very red or complex objects or bright standard stars through another filter. The normal acquisition procedure is capable of identifying objects with H<15 in a single direct image. For fainter objects, sky subtraction can be used (see Figure 2). This permits identification of objects with H<18.5. For still fainter objects, direct imaging is still possible in theory, but increasingly time consuming; the preferred method is instead to acquire a nearby point source and then to do a precision offset using one of the telescope's peripheral wavefront sensors (PWFS). This requires accurate knowledge of the required offset. The best results are obtained when the reference star is within an arcminute or so of the science target; the nominal error for offsets up to 50 arcsec is <0.2 arcsec.

2.1.2 Observation

Once the object is centered, the acquisition mirror is removed from the beam and the instrument is ready for the science observation. The telescope is then offset slightly, normally to move the object a small amount along the slit, and the first exposure is taken. The telescope is then offset again, another exposure is taken, and so on until the desired total integration time is accumulated.

For point sources, or objects of very small spatial extent, the normal practice is to alternate between two positions on the slit, but one can get somewhat better sky removal and flat-fielding performance if more positions are used. This is easier to do in the long slit mode, since the cross-dispersed slit is quite short (6 arcsec), so it is hard to fit more than two positions, especially in worse than average seeing (see Figure 3, lower right image). In long slit mode, the 99 arcsec slit length allows one to dither "on-source" even for fairly extended objects.

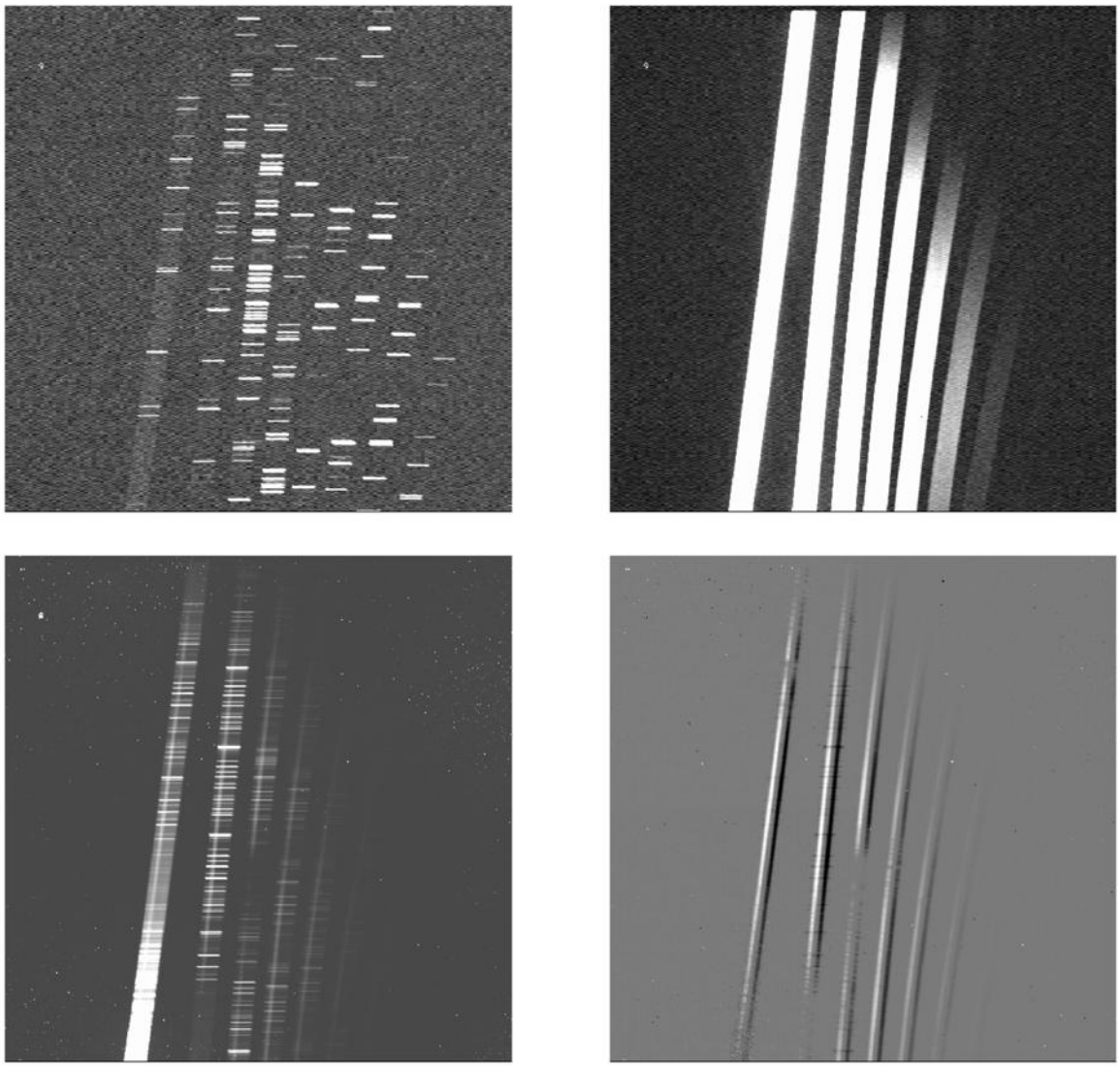

Figure 3. Examples of data in the cross-dispersed mode. The top images are calibration data: Ar lamp spectrum (top left) and a quartz-halogen lamp spectrum (top right). The bottom left exposure is a 5 minute exposure on a star with K~13.5, J-K~1.1. The bottom right exposure is the difference between the image on the left and a second image taken with the telescope offset by approximately 3 arcsec along the slit. Note the incomplete subtraction of the strongest night sky lines in the difference image. The spectra are successive grating orders, starting with order 3 on the left, which corresponds approximately to K band. Wavelength decreases to the right, with increasing order, and increases within an order toward the bottom of the images. The stellar spectrum is visible in the difference image down to around 0.8 μm.

2.1.3 Calibrations

Two types of calibrations are normally taken: standard stars and calibration unit lamps. The standard star is a relatively bright star that is observed at approximately the same airmass as the science target, which is used to remove absorption features from the terrestrial atmosphere. Usually, but not always, early-type stars are used, as these have only a few intrinsic spectral features, which can be corrected for. The acquisition and observation procedures for these standard stars are the same as for science targets, though obviously much quicker to execute.

The calibration unit observations comprise flat field observations of a continuum source, which are used to remove pixel-to-pixel variations in the instrument response. Because of the broad wavelength coverage of the cross-dispersed mode, obtaining suitable flat-field illumination across all orders has proved challenging. A broader, near-infrared "balance" filter has been added to the Gemini calibration unit that has improved the situation considerably. Still, at present two lamp-plus-filter configurations are used to properly illuminate all of the orders .In addition, an arc lamp spectrum is usually taken, although in most cases the night sky lines in the science target and standard star observations are sufficient to provide wavelength calibration. An example of each type of calibration unit spectrum is shown above (Figure 3).

2.2 Throughput and sensitivity

Two main factors affect GNIRS's sensitivity: system throughput and detector properties. Performance may also be affected by additional factors such as stray light and ghost images, but the design was generally quite successful in eliminating such problems.

2.2.1 System throughput

The throughput for the system – atmosphere, telescope, and instrument, including the detector - was estimated during the design phase using predicted values for component performance. During integration, these values were revised using measured values for component performance where possible, and witness samples or representative data where direct measurements were not available. These estimates are listed as "designed" and "predicted as-built" system performance respectively in Table 1, for some representative instrument configurations. The differences between the "designed" and "predicted as-built" values are mainly due to the reduced efficiency of the 32 l/mm grating ruling, compared with an ideal grating.

The throughput was also measured at the telescope. The measurements were made on stars of known brightness using a very wide slit to eliminate light losses at the slit. The results of these measurements are also given in Table 1.

Table 1. GNIRS throughput calculations and measurements

GNIRS configuration (Short camera)	Designed system throughput	Predicted as-built system throughput	Measured system throughput
32 l/mm, 1.27 μm	29%	18%	11%
32 l/mm, 1.64 μm	40%	25%	21%
32 l/mm, 2.22 μm	39%	24%	19%
110 l/mm, 1.27 μm	25%	25%	16%
110 l/mm, 2.22 μm	36%	33%	24%

The H and K measurements are close to the predictions, although systematically lower. The measurements at 1.27 μm are quite a bit lower, which appears mainly to be because the true instrument response at this wavelength is quite a bit off the peak of the blaze for this order. Note that these are, in all cases, system throughput, which includes the atmosphere and telescope. The throughput of the instrument alone would be ~15% higher than the system throughput.

By way of comparison, the measured throughput in the acquisition mode, with the short camera and a 2.12 μm narrowband filter, is about 25%.

2.2.2 Detector properties

The GNIRS science detector is an ALADDIN III 1k x 1k InSb array. General properties of the arrays furnished to Gemini are discussed in [5]. The array controllers are discussed in [3]. The specific array used in GNIRS has very good cosmetic performance (see Figures 2-4).

Although much of the initial array testing was done at temperatures of 30K or above, we found that best performance was achieved by cooling the detector to 28-29K. At these temperatures, dark current measured on long (10-20 minute) exposures was <0.1 electrons/sec/pixel, typically ~0.05 electrons/sec/pixel.

The measured read noise for a single detector read is ~40 electrons, but can be reduced using multiple non-destructive reads ("Fowler sampling"[11]). We have been able to reduce the effective read noise to close to 5 electrons, at the telescope, using a large number of samples. The reduction in read noise at this point is offset by the relatively long overheads associated with the samples, so in practice the lowest-noise mode used is one offering ~7 electrons read noise and 18 seconds of read overhead. Measured dark current at the telescope is <0.1 electrons/sec/pixel for exposures of ~20 minutes.

The detector also shows low-level residual images, which affect instrument performance in certain circumstances, specifically after observing flat fields or acquisition images, or over-exposing bright calibration stars. Residual images can be seen at a low level in long, low-background exposures for an hour or so after a saturated image was taken. The residual effects of the acquisition images are minimized by co-adding several short exposures rather than taking an equivalent longer exposure. The flat field effects are minimized by doing calibrations at the end of the night where possible.

2.2.3 Cosmic rays

During the late stages of integration and testing, we discovered that the configurations using the short-focus cameras [2] had a significant excess of "cosmic ray" events, which were traced to the use of thorium fluoride in the anti-reflection coatings on the camera lenses. The particles producing these events have relatively low energy, and were only produced by configurations where there was a direct path from the last lens surface to the detector. The solution to the problem was to replace the final lenses in the short-focus cameras by lenses with non-radioactive anti-reflection coatings. This replacement was carried out in mid-2005; the resulting reduction in "cosmic rays" is shown in Figure 4 (the data in Figure 3 also post-date the lens replacement).

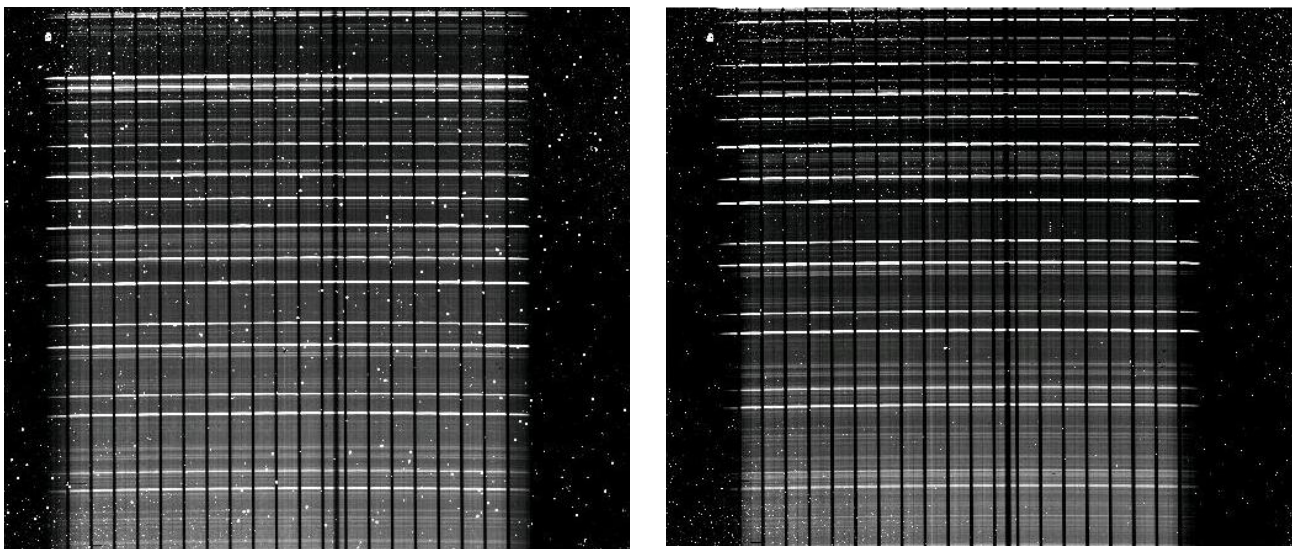

Figure 4. Effects of radioactive lens coating. The images were both taken in K band with the IFU[7] at R~6000, at slightly different center wavelengths. The left-hand image was taken before the lens replacement and the right-hand image was taken afterward. Exposure times were 10 minutes for the left-hand image and 15 minutes for the right-hand image.

As part of the effort during the lens replacement, the blocking filter for the cross-dispersed mode was also replaced. The original filter was specified to restrict transmission to the region between 0.85 and 2.5 μm, but tests showed that a less-restrictive bandpass did not result in detectable scattered light. The new filter is limited to blocking wavelengths beyond

~4 μm. The overall transmission is better by 10-20% over the 0.9-2.4 μm region. At shorter wavelengths the instrument performance is limited primarily by the gold coatings used on the mirrors. Comparable images taken with the old and new filters are shown below (Figure 5).

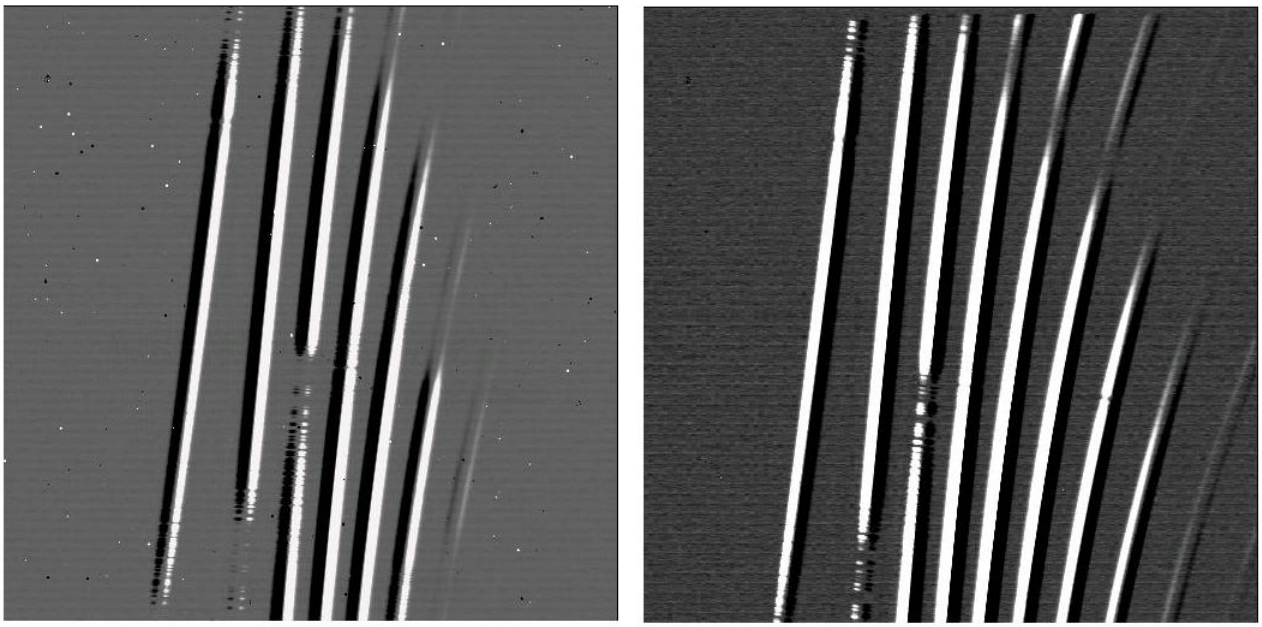

Figure 5. Replacement of cross-dispersed blocker. Difference spectra are shown with the old filter (left) and new filter (right). Spectrum layout as in Figure 3. The stars were both of spectral type A0 with exposures set to give comparable counts. The old filter cuts off around 0.8 μm (middle of order 8); with the new filter the stellar flux starts to decrease around 0.7 μm (order 9).

2.2.4 Optimizing performance

The optimum use of GNIRS depends significantly on the specifics of the science program. However, several general principles apply:

- The use of Fowler sampling[11] improves performance for observations of faint objects and low background, requiring integration times of several minutes or longer. For brighter objects or high background the added read overheads are better used for more integration.
- Maximum integration times are usually set by the background; it is usually a good idea to avoid saturating strong emission lines since they produce residual images. However, at the shortest wavelengths it is in principle possible to integrate for tens of minutes. This is not recommended because the night sky will vary significantly, and these variations will dominate read noise or photon statistics (see Figure 3).
- Because nearly all observations are background-limited, a very wide slit can result in reduced signal to noise. A wider slit also reduces spectral resolution. However, a wider slit (~0.68 arcsec) is recommended for objects acquired by blind offsets (see 2.1.1) to accommodate the uncertainties in centering on the slit.
- The "dithering" on the slit can be optimized for the specific program, slit length, and expected image quality.

Other suggestions for optimizing observing programs can be found at the GNIRS web site[10]. An integration time calculator is available for GNIRS[12], which allows one to compare the performance for different instrument configurations.

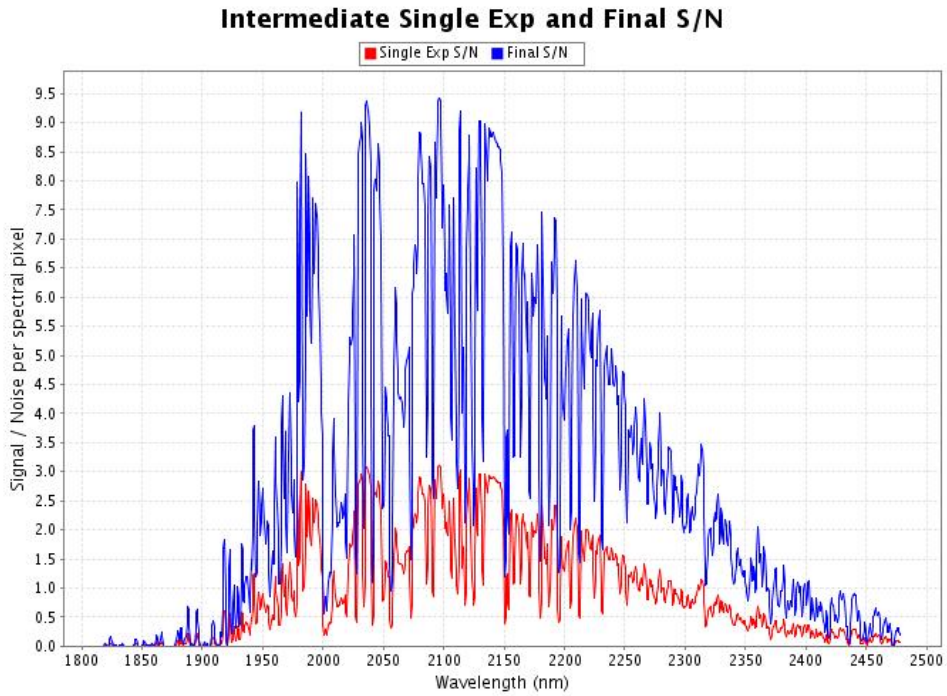

Figure 6. Example of GNIRS integration time calculator output. The figure shows the predicted signal to noise for a K=19 point source under median conditions, at R=1700 with the short camera. The detector is in the read mode for very faint objects (32 Fowler samples.) The lower curve is for a single 10-minute exposure while the upper curve is for 3 hours total integration time. Most of the structure is produced by emission lines in the Earth's atmosphere, which increase background and therefore reduce signal to noise. The reduced signal to noise near 2.00 and 2.05 μm, as well as some structure at the red end of the band, is due to absorption from terrestrial CO_2 and H_2O. See [12] for details.

Actual observations (e.g, [13-18]) confirm the predictions of the integration time calculator.

2.3 Other aspects of GNIRS performance

2.3.1 Flexure

While observing, GNIRS relies on either the peripheral wave-front sensors or the OIWFS to maintain the target centered on the slit. Since the OIWFS is located within GNIRS, flexure of the instrument structure as a whole is compensated, and guiding is in principle very accurate. The only residual effects are structural flexure within the GNIRS optical bench, and flexure of the OIWFS mechanisms and the GNIRS slit. These are quite small, as shown in Figure 6. However, the OIWFS detector system is not currently offered, as it does not at present work at the bandwidth and sensitivity required to provide full tip-tilt correction. This implies that for best performance one would need to work with the PWFS for tip-tilt correction and the OIWFS for flexure correction. This involves additional observing overheads, and it is not clear at present whether these would offset the time saved by reducing the frequency of re-centering during long observations.

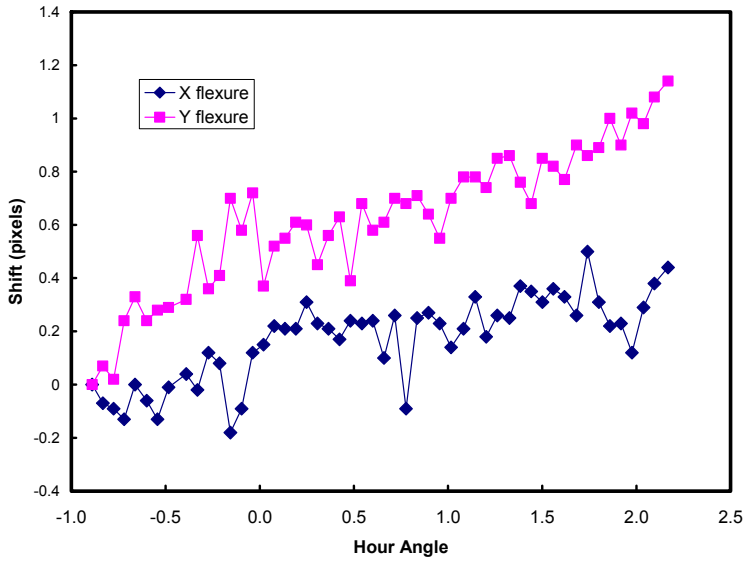

Figure 7. Flexure of slit relative to OIWFS, in pixels as the telescope tracks in hour angle. The shift over ~3 hours is about 0.2 arcsec.

Flexure when using the PWFS is substantially larger, although still quite acceptable. This is because the PWFS are located inside the instrument rotator, so flexure of the GNIRS structure relative to the mounting surface is relevant. Measured flexure values are typically 0.3 arcsec/hour or less.

2.3.2 Reliability

GNIRS has proven to be a very reliable instrument at the telescope. With the exception of the scheduled upgrade mentioned in 2.2.3, GNIRS has not had any significant downtime in nearly 2 years of continuous operation. The scheduled work included not only the camera lens replacements, but also installation of 3 new filters and overhaul of all 4 cold-heads, which is necessary approximately every 10,000 hours of operation. The filters comprised two narrowband filters for acquisition using emission features at 2.12 and 3.29 μm, and the new blocking filter for the cross-dispersed mode described above. The mechanisms, and in particular the cryogenic motors, have worked exceptionally well since commissioning. Total time loss due to instrument problems is approximately 2% of total instrument time on-sky, and the majority of this has been related to software and electronics associated with the detector controller, network issues, or occasionally instrument sequencer software (see [19]).

2.3.3 Data reduction

A dedicated data reduction package is available for GNIRS data as part of the Gemini IRAF package[20].

3. OPERATIONAL EXPERIENCE

3.1 Science demand

After its initial commissioning, GNIRS has seen extensive use on the telescope, averaging 20-25% of the science time at Gemini South since it began regular observations. In the last three semesters (2005B-2006B), it has been the most popular infrared instrument at Gemini, based on fraction of time requested in proposals. GNIRS has proven to be a very flexible instrument in terms of observing conditions since the majority of the science is not dependent on sky background, and many programs can be done with less than optimal cloud cover and image quality. This is important for the nominal multi-instrument queue observing now carried out at Gemini, and means that GNIRS programs enjoy a

high completion rate in the queue. To date, there have been 6 refereed publications resulting in whole or in part from data taken with GNIRS[13-18].

Of the various modes provided by the specifications in section 1, some are significantly more popular than others:

- The most-used mode is the cross-dispersed mode (R~1700 over 0.8-2.5 μm), which accounts for nearly half of current use and five of the six publications thus far (the sixth is based on IFU data). This mode sees a lot of use from the extra-galactic community for observations at both moderate ($2<z<3$) and high red-shift where the extended wavelength coverage is important to detect multiple lines for firm red-shift identification and follow-up analysis (e.g., [13]). The improved blue response at and below 1 μm with the new cross-dispersed blocker installed in mid-2005 (see 2.3.2) is especially good news for "high-z" (redshift>7) galaxy hunters ([16]).
- The long-slit mode with the 0.15 arcsec pixels is used primarily for extended objects at 1-2.5 μm and occasionally for observations between 3 and 5 μm.
- The integral field unit has been used between 1 and 2.5 μm to observe compact objects such as young binaries and the cores of galaxies ([15]). It is can be used between 3 and 5 μm, but so far no science programs have used it at these wavelengths.
- In addition, some investigators have taken advantage of the cross-dispersed mode at high resolution (R~6000), which provides incomplete coverage of multiple orders.
- GNIRS has seen very little use beyond 2.5 μm so far, and only occasional use of the R=18,000 mode with the long (0.05 arcsec/pixel) cameras, which is currently limited to very bright targets because of the substantial slit losses. The polarization mode is not offered as it requires the Gemini polarization unit (GPOL), which is not available. In addition, the lowest resolution mode and the cross-dispersed mode with the 0.05 arcsec pixel scale are not offered at this time due to the limited usefulness of the long cameras without adaptive optics.

3.2 Lessons for future instruments

Several aspects of our experience should be taken into account in the design of future instruments:

- The instrument specifications were optimized for use in the best conditions expected at the telescope. In practice, these arise infrequently (photometric conditions with 20th percentile image quality occur about 10% of the time). As a result, most programs adopt slit widths of 3 or more pixels. A pixel size of 0.20 or 0.25 arcsec would probably have been preferable (compare [21]). This would have provided a better combination of spectral resolution and coverage while still providing good performance under all but the most extraordinary conditions.
- The variety of modes potentially available certainly added to the complexity (and cost) of GNIRS. In addition, the need to provide support for whatever modes are offered for use has led the Gemini Observatory to limit the selection of what is available: one grating, and two prisms are not currently offered for use. The second IFU position is not used, as that IFU was not built, though this drove the overall size of the mechanism. The long 3-5 μm camera, though available, has not been used for date for a science program. It is worth noting that a single, fixed configuration (cross-dispersed 0.9-2.5 μm) represents about half the science use of GNIRS, and that such a fixed format instrument would have been inexpensive and reliable. It is also worth noting, though, that the original prioritization of capabilities[1] did not anticipate this. What this suggests is that it is worthwhile trying to reduce the number of modes in an instrument – more is not always better – but at the same time it is important to recognize that predicting science demand several years in the future can be difficult. The long-camera modes were intended in large part for use in combination with an adaptive optics system, which may occur in the future.
- Although the "acquisition mirror" was intended to facilitate acquisition and recentering by avoiding the need to move dispersing elements, there are still some mechanism motions involved and the residual image from the acquisition process can be a nuisance. A still better solution would have been a reflective slit, similar to that in NIRSPEC[22]. This would also have assisted with the difficult task of centering very faint objects (see 2.1.1). Even so, the capability provided makes possible acquisition of very faint objects and enables science that could not be carried out with a more rudimentary capability.

Overall, GNIRS has proved to be a very successful instrument. Aside from the publications noted above, this is also indicated by increasing demand. Most Gemini instruments are available in both "classical" and "queue" modes; it is worth noting that GNIRS sees a significant demand for use in “classical” mode which implies that users have found it to be easy and efficient to use.

ACKNOWLEDGEMENTS

Portions of this paper are based on observations obtained at the Gemini Observatory, which is operated by the Association of Universities for Research in Astronomy, Inc., under a cooperative agreement with the NSF on behalf of the Gemini partnership: the National Science Foundation (United States), the Particle Physics and Astronomy Research Council (United Kingdom), the National Research Council (Canada), CONICYT (Chile), the Australian Research Council (Australia), CNPq (Brazil) and CONICET (Argentina). NOAO is operated by the Association of Universities for Research in Astronomy, Inc. (AURA) under cooperative agreement with the National Science Foundation.

We are also grateful to the many NOAO and Gemini staff members who helped with successful commissioning of this instrument, and to the Gemini and National Gemini Office staff who have provided continuing support for science observations with GNIRS at Gemini South.

REFERENCES

1. Mountain, M., “A Scientific Perspective on the Requirements for the 1-5 Micron Spectrograph,” *Gemini Technical Note* TN-PS-G0020 (1994).
2. J. H. Elias, R. R. Joyce, M. Liang, G. P. Muller, E. A. Hileman, and James R. George, “Design of the Gemini near-infrared spectrograph,” *Proc. SPIE* 6269-160 (2006).
3. K. W. Hodapp, J. B. Jensen, E. M. Irwin, H. Yamada, R. Chung, K. Fletcher, L. Robertson, J. L. Hora, D. A. Simons, W. Mays, R. Nolan, M. Bec, M. Merrill, and A. M. Fowler, “The Gemini Near-Infrared Imager (NIRI),” *PASP* 115, 1388 (2003).
4. K.-W. Hodapp, E. M. Irwin, H. Yamada, R. Chung, K. Fletcher, J. Jensen, W. Mays, R. Nolan, D. A. Simons, and C. Aspin, “Gemini near-infrared imager (NIRI): a discussion of its design features and performance,” *Proc. SPIE* 4841, 869 (2003).
5. W. Harrison, A. M. Fowler, and W. Ball, "Characterization of Gemini near-IR arrays,” *Proc. SPIE* 3354, p. 214 (1998).
6. M. Dubbeldam, R. Content, J. R. Allington-Smith, S. Pokrovki, and D. J. Robertson, “Integral field unit for the Gemini near-infrared spectrograph,” *Proc. SPIE* 4008, 1181 (2000).
7. J. R. Allington-Smith, C. M. Dubbeldam, R. Content, C. J. Dunlop, D. J. Robertson, J. Elias, B. Rodgers, and J. E. Turner, “Integral field spectroscopy with the Gemini Near-Infrared Spectrograph,” *Proc. SPIE* 5492, 701 (2004).
8. D. Vukobratovich, K. Don, and R. E. Sumner, “Improved cryogenic aluminum mirrors,” *Proc. SPIE* 3435, 9 (1998).
9. E. A. Hileman, J. Elias, R. Joyce, R. Probst, M. Liang, and E. Pearson, “Passive compensation of gravity flexure in optical instruments,” *Proc. SPIE* 5495, 622 (2004).
10. Gemini staff, http://www.gemini.edu/sciops/instruments/nirs/nirsIndex.html
11. A. M. Fowler and I. Gatley, “Noise reduction strategy for hybrid IR focal-plane arrays,” *Proc. SPIE* 1541, 127 (1991).
12. Gemini staff, http://www.gemini.edu/sciops/instruments/itc/ITCgnirs.html
13. P. G. van Dokkum, M. Kriek, B. Rodgers, M. Franx, and P. Puxley, “Gemini Near-Infrared Spectrograph Observations of a Red Star-forming Galaxy at z=2.225: Evidence of Shock Ionization Due to a Galactic Wind,” *ApJ.* 622, L13 (2005).
14. K. L. Luhman, D.E. Peterson, and S. T. Megeath, “Spectroscopic Confirmation of the Least Massive Known Brown Dwarf in Chamaeleon,” *ApJ*, 617, 565 (2004).
15. J.D. Silge, K. Gebhardt, M. Bergmann, and D. Richstone, “Gemini Near Infrared Spectrograph Observations of the Central Supermassive Black Hole in Centaurus A,” *AJ*, 130, 406 (2005).
16. B. Mobasher, M. Dickinson, H. C. Ferguson, and 27 others, “Evidence for a Massive Post-starburst Galaxy at z~6.5,” *ApJ*, 635, 832 (2005).

17. K. L. Luhman, L. Adame, P. D'Alessio, N. Calvet, L. Hartmann, S.T. Megeath, and G. G. Fazio, "Discovery of a Planetary Mass Brown Dwarf with a Circumstellar Disk," *ApJ*, 635, L93 (2005).
18. M. Kriek, P. van Dokkum, M. Franx, N.F. Schreiber, E. Gawiser, and 9 others, "Direct Measurements of the Stellar Continua and Balmer/4000 Angstrom Breaks of Red z>2 Galaxies: Redshifts and Improved Constraints on Stellar Populations," *ApJ*, accepted (2006).
19. C. D. Guzman and E. Zarate, "Modeling the costs of developing and supporting detector controllers in a multi-instrument observatory," *Proc. SPIE* 6271-43 (2006).
20. A. Cooke and B. Rodgers, "IRAF Package for GNIRS Data Reduction -- A Product of the Gemini/NOAO Collaboration," *ASP Conf Series*, 347, 514 (2005).
21. M. Liang, R. R. Joyce, S. S. Eikenberry, K. H. Hinkle, G. P. Muller, J. Ge, and D. Sprayberry, "Optical design of the high-resolution near-infrared spectrograph," *Proc. SPIE* 6269-162 (2006).
22. I. S. McLean, J. R. Graham, E. E. Becklin, D. F. Figer, J. F. Larkin, N. A. Levenson, and H. I. Teplitz, "Performance and results with the NIRSPEC echelle spectrograph on the Keck II telescope," *Proc. SPIE* 4008, 1048 (2000).